

## RESEARCH ARTICLE

# Hydroclimatic and ecohydrological resistance/resilience conditions across tropical biomes of Costa Rica

Germain Esquivel-Hernández<sup>1</sup>  | Ricardo Sánchez-Murillo<sup>1</sup> | Christian Birkel<sup>2,3</sup> | Stephen P. Good<sup>4</sup> | Jan Boll<sup>5</sup>

<sup>1</sup>Stable Isotope Research Group, Chemistry Department, National University of Costa Rica, Heredia, Costa Rica

<sup>2</sup>Department of Geography, University of Costa Rica, San José, Costa Rica

<sup>3</sup>Northern Rivers Institute, University of Aberdeen, Aberdeen, UK

<sup>4</sup>Department of Biological and Ecological Engineering, Oregon State University, Corvallis, OR, USA

<sup>5</sup>Department of Civil and Environmental Engineering, Washington State University, Pullman, WA, USA

## Correspondence

Germain Esquivel-Hernández, Universidad Nacional de Costa Rica, Campus Omar Dengo, P.O. Box 86-3000, Heredia, Costa Rica.  
Email: germain.esquivel.hernandez@una.cr

## Abstract

Water resources management in the tropics is challenged by climate variability and unregulated land use change and their impacts on the complex interactions between vegetation, soil, and atmosphere. This study focuses on the analysis of hydroclimatic and ecohydrological conditions across 6 major biomes in Costa Rica. Using the Budyko and the Tomer–Schilling frameworks, 31 reanalysis data points located across the Caribbean and Pacific domains were classified according to their ecohydrological resistance and resilience between 1989 and 2005. Observed data were used to evaluate the reanalysis products. Resistance was defined as the standard deviation in the water excess ( $Q/P$ ), whereas resilience was defined as the standard deviation of the energy ( $AET/PET$ ) to the water excess. A strong orographic separation was obtained between the water-limited Pacific slope and the energy-limited Caribbean slope. The Caribbean slope is characterized by low resistance and high resilience to changes in the hydroclimatic conditions, with small relative changes in water excess (−18% to 2.0%), whereas the Northern Pacific slope has high resistance and low resilience and exhibited strong changes in water excess (−34% to 0%). Some regions of the Northern Pacific region covered by lower and premontane forests have recently suffered significant increments in the dryness index ( $PET/P$ ). This study demonstrates the need for national–regional strategies to effectively optimize water use efficiency and water storage and to include a climate vulnerability component in future water management plans.

## 1 | INTRODUCTION

The scientific community generally agrees that the Earth's climate is experiencing changes in response to inherent natural variability and increasing greenhouse gas and aerosol concentrations, which may affect sensitive and complex ecosystem assemblages in the tropics (Giorgi, 2006; Karmalkar, Bradley, & Diaz, 2011). In tropical regions such as Central America, climate change is influencing water vapor mixing ratio distributions, cloud formation mechanisms, precipitation, and runoff patterns (Hidalgo, Amador, Alfaro, & Quesada, 2013; Maurer, Adam, & Wood, 2009). This change appears to affect variability in hydrological conditions on the wet and dry end of the spectrum (Giorgi, 2006). Therefore, quantitative information is needed related to water budgets, both temporally and spatially, and the implications of the climatic changes over a wide range of ecosystems and socioeconomic activities (Imbach et al., 2010; Maldonado, Alfaro, Fallas-López, & Alvarado, 2013).

Tropical ecohydrological conditions are usually under the influence of complex land–ocean–atmosphere interactions that produce a

dynamic cycling of mass and energy. This cycling is affected mainly by soil moisture dynamics, sea surface temperature, vegetation cover, and the seasonality of the rainfall regime (Alfaro, 2002; Fisher et al., 2009; Wohl et al., 2012). These interactions result in distinct precipitation and runoff regimes that generate a notable difference in biomes across landscapes (Imbach et al., 2010). Overall, forested ecosystems are rapidly and directly being transformed due to land use changes of expanding human populations and economies, including locations inside protected areas (Allen, Macalady, Chenchouni, Bachelet, & McDowell, 2010). Precipitation patterns are also expected to be severely affected by deforestation in tropical areas, which could lead to a strong impact on the local and regional mean water balance (Hassler, Werth, & Avissar, 2009). Consequently, information related to changes in the hydroclimatic conditions due to alterations in forest cover is needed to develop effective water and wildlife management plans (De Fries, Karanth, & Pareeth, 2010).

Future land use scenarios indicate that shifts in the distribution of tropical forest life zones are likely to occur because of climatic changes (Enquist, 2002; Feeley, Hurtado, Saatchi, Silman, & Clark, 2013).

However, the responses to climatic drivers of tropical biomes have not been studied in great depth. Understanding of these responses, therefore, is important to shape the role of tropical forests in global carbon and hydrological cycles (Allen et al., 2010; Chazdon, Redondo-Brenes, & Vilchez-Alvarado, 2005).

The estimation of changes in the ecohydrological functional properties of catchments such as hydrologic connectivity, seasonality, memory, and synchronicity may be used to integrate landscape features with spatiotemporal processes and patterns and their hydrologic functioning (i.e., water storage and discharge; Carey et al., 2001). In this context, two functional properties of catchments can be taken from ecology theory and transformed into ecohydrological properties (Tomer & Schilling, 2009): resistance and resilience. Resistance measures the degree to which runoff is coupled/synchronized with precipitation, and resilience measures the degree to which a catchment can return to normal functioning following perturbations from events, for example, a drought, deforestation, or a precipitation increase (Carey et al., 2001; Creed et al., 2014).

In order to quantify hydrological changes at regional to global scales, the Budyko framework is useful to predict the mean annual water availability as a function of regional dryness and to estimate the hydroclimatic changes induced by natural and human factors (Budyko, 1974; Tekleab et al., 2011; van der Velde et al., 2013; Greve, Gudmundsson, Orlowsky, & Seneviratne, 2015). The Budyko framework was recently used to examine the change in forest land use and water yield in response to climate warming across North America (Creed et al., 2014), interpret the role of water balances in arid regions (Du, Sun, Yu, Liu, & Chen, 2015), analyze vegetation dynamics significance in the analysis of hydroclimatic conditions at small spatiotemporal scales (Donohue, Roderick, & McVicar, 2007), and assess the hydrological conditions beyond the steady-state assumption in closed terrestrial water balances (Greve et al., 2015).

Traditionally, high data availability in northern temperate regions has allowed a robust analysis of hydroclimatic conditions at regional scales. In tropical regions, however, climate observation networks are sparse and unevenly distributed (Worqlul et al., 2015) and the regional scale of water distribution is still poorly understood. This lack of information has opened new opportunities for the use of satellite estimations in regions with limited or no conventional ground observations. Likewise, recent analyses highlight the need to estimate the accuracy and precision of these observations using on-the-ground data (Misra, Pantina, Chan, & DiNapoli, 2012; Fuka et al., 2013; Worqlul et al., 2015). In addition, besides climate, land use change is an important driver in watershed hydrology; yet their relative effects are difficult to separate empirically (Findell & Knutson, 2006; Tomer & Schilling, 2009; Zhang, Yang, Yang, & Jayawardena, 2015). In this sense, the conceptual model proposed by Tomer and Schilling (2009) can separate climatic from land use effects on the water balance, using a coupled water–energy budget in order to distinguish relative impacts of climate and land use change on regional hydrology (Peña-Arancibia et al., 2012; Renner, Seppelt, & Bernhofer, 2012).

In this work, the Budyko (1974) and Tomer–Schilling (2009) frameworks were used to analyze the hydroclimatic conditions and their influence on the ecohydrological resistance and resilience across six different biomes of Costa Rica between 1989 and 2005. The

analysis is based on climate reanalysis data, land evapotranspiration products, and observed precipitation and runoff. The main objectives of this study were to (a) evaluate the Pacific and Caribbean slopes according to how closely average annual values fall onto the Budyko curve; (b) estimate the spatial distribution of ecohydrological resistance and resilience based on the Tomer–Schilling framework and its relation to major biomes; and (c) analyze to what extent changes in land cover and climatic variability lead to overall positive or negative deviations in the hydrological conditions.

## 2 | MATERIAL AND METHODS

### 2.1 | Regional characteristics

Costa Rica is located in the tropics between 8°–11°N latitude and 82°–86°W longitude. A mountain range divides the country into two main climate regions, the Pacific and Caribbean slopes (Figure 1a), which are lee and windward, respectively, in relation to the North Atlantic trade winds, the dominant wind regime (Maldonado et al., 2013). These climate regions are influenced by four regional air mass circulation processes: northeast trade winds, the latitudinal migration of the Intertropical Convergence Zone, cold continental outbreaks, and sporadic influence of tropical cyclones (Waylen, 1996). These circulation processes produce a distinct circulation pattern across the country. During the wet season (May–November), the air masses arriving in Costa Rica can be classified as continental winds, reaching Costa Rica from the Pacific Ocean. In the dry season (December–April), trade winds bring air masses from the Caribbean Sea. The influence of the wind circulating patterns is also observed in the Pacific precipitation regime, resulting in two rainfall maxima, one in May–June and one in September–October, which are interrupted by a relative minimum between July and August known as the Midsummer Drought (i.e., intensification of the trade winds over the Caribbean Sea; Magaña, Amador, & Medina, 1999; Saénz, & Durán-Quesada, 2015). Annual precipitation varies from ~1,500 mm in the northwestern region to ~7,000 mm on the Caribbean slope of the Talamanca Cordillera. Temperature seasonality is low. The mean annual temperatures (MATs) vary from around 27 °C on the coastal lowlands, to 20 °C in the Central Valley, and below 10 °C at the summits of the highest mountain range (Sánchez-Murillo et al., 2013).

Costa Rica's high biodiversity (comprising ~4% of the global biodiversity; <http://www.inbio.ac.cr/conservacion.html>) is protected under a successful conservation program (known as the National System of Conservation Areas, SINAC, <http://www.sinac.go.cr>). This protection and conservation scheme allows Costa Rica to preserve ~48% of forested areas of which 43% are within protected areas such as national parks and biological reserves (Sánchez-Azofeifa, Calvo-Alvarado, Chong, Castillo, & Jiménez, 2006; Sánchez-Azofeifa et al., 2002). Biomes in Costa Rica are influenced by the precipitation, temperature, and evapotranspiration regimes and their location on either the Caribbean or the Pacific slopes. Following the life zone classification developed by Holdridge (1978), vegetation cover ranges from seasonally dry forests in the Northern Pacific region, where fine-leaved trees of the legume family are common, to increasingly moist and wet habitats that change to perpetual montane wet or rain

(cloud) forests above 1,800 m a.s.l, where trees are tall and species such as the kapok (*Ceiba pentandra*) and espavé (*Anacardium excelsum*) are common. In upper montane forest (1,500–2,000 m a.s.l), tall trees and dense canopy are widespread, whereby oak (genus *Quercus*) and alder (*Alnus*) are abundant (Condit, Pérez, & Daguerre, 2010; Powell, Barborak, & Rodríguez, 2000). Further east, the Caribbean rainforests show a moderate dry season of 1–2 months. A secondary gradient exists along the Pacific coast where wetness increases from north to south (Powell et al., 2000). Together, precipitation, vegetation, and solar radiation, much of it being diffuse due to high degree of cloud cover, lead to relatively high annual actual evapotranspiration (AET) rates of around 1,000 mm (Imbach et al., 2010), with transpiration rates up to 60% of this rate (Rhodes, Guswa, & Newell, 2006).

## 2.2 | Data description

The analysis of ecohydrological conditions used two primary data sets. First, precipitation (P) and potential evapotranspiration (PET) was taken

from the multiyear gridded Climate Forecast System Reanalysis (CFSR) computed by the National Center for Environmental Prediction for years 1979–2013 (Saha et al., 2010). Second, daily CFSR data (P, wind speed, relative humidity, and solar radiation) were obtained from the Texas A&M University website (<http://globalweather.tamu.edu>). For Costa Rica, the CFSR data set consists of a collection of 46 reanalysis estimated data or sites (hereafter sites) across five climate regions, with a spatial resolution of ~38 km (Figure 1a and Table 1). A secondary data set was the LandFlux-EVAL estimated AET (Mueller et al., 2013), which is available for the time period 1989–2005, and it is interpolated to a unified 1° grid size. This data set was used to estimate the AET across Costa Rica. The spatial coverage of the LandFlux-EVAL AET data includes 31 sites out of the 46 CFSR sites calculated by the climate reanalysis.

## 2.3 | Raw data processing and evaluation

We selected 31 CFSR sites for the analysis of the ecohydrological conditions in the time period 1989–2005. This time period was selected

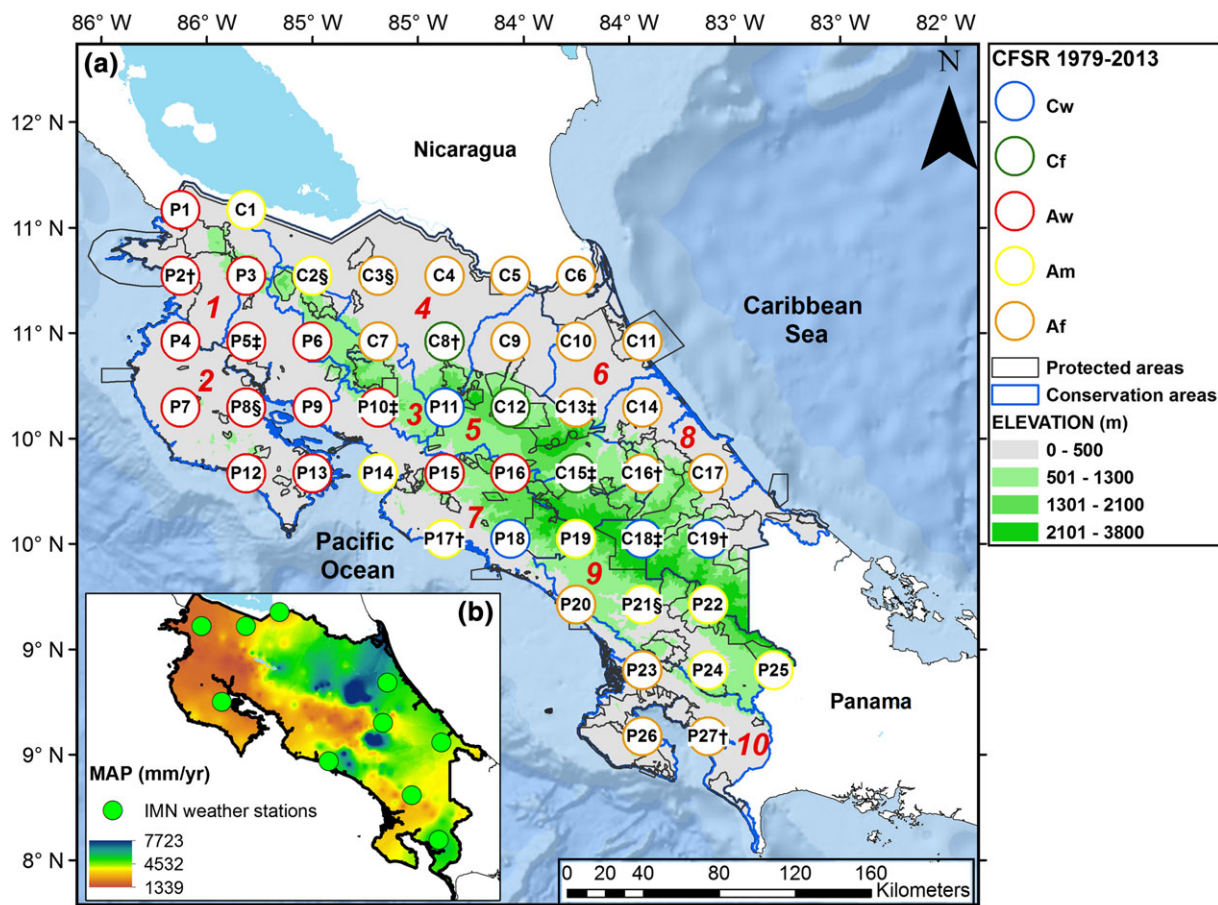


**FIGURE 1** (a) Spatial distribution of 46 CFSR estimates available for Costa Rica between 1979 and 2013. Estimates were consecutively labeled based on their location in the Pacific slope (P) or in the Caribbean slope (C). Selected CFSR estimates were classified as follows: S: CFSR estimates evaluated using in situ P, PET, and AET data, †: CFSR estimates evaluated using in situ P and PET data, and ‡: CFSR estimates evaluated using in situ AET data. They were also categorized according the Köppen–Geiger climate classification (Kottek et al., 2006) described in Table 1. Conservation (blue polygons) and protected (black polygons) areas are also shown in the map. Conservation areas were numbered in red according to the following description: (1) Guanacaste Conservation Area, (2) Tempisque Conservation Area, (3) Arenal-Tempisque Conservation Area, (4) Arenal Huertar Norte Conservation Area, (5) Central Volcanic Conservation Area, (6) Tortuguero Conservation Area, (7) Central Pacific Conservation Area, (8) La Amistad-Caribe Conservation Area, (9) La Amistad-Pacifico Conservation Area, and (10) Osa Conservation Area. (b) The inset map shows the mean annual precipitation (MAP, mm/year) calculated for Costa Rica (Sánchez-Murillo & Birkel, 2016). The IMN weather stations used for the in situ evaluation of the CFSR data are also shown (green circles). CFSR = Climate Forecast System Reanalysis; P = precipitation; PET = potential evapotranspiration; AET = actual evapotranspiration; IMN = National Meteorology Institute of Costa Rica

**TABLE 1** Summary of the CFSR sites characteristics available for Costa Rica between 1979 and 2013

CFSR estimate code	Longitude (decimal degrees)	Latitude (decimal degrees)	Elevation (m a.s.l.)	Climate type and location <sup>a</sup>	Watershed	Holdridge life zone <sup>b</sup>
C1	-85.313	11.084	139	Am	Orosí	wf-T
C2	-85.000	10.772	340	Am	Zapote	wf-T
C3	-84.688	10.772	59	Af	Frío	mf-T
C4	-84.375	10.772	72	Af	San Carlos	wf-PM
C5	-84.063	10.772	26	Af	Sarapiquí	wf-T
C6	-83.750	10.772	2	Af	Chirripó	wf-T
C7	-84.688	10.460	745	Af	Pocosol	wf-PM
C8	-84.375	10.460	98	Cf	San Carlos	wf-PM
C9	-84.063	10.460	108	Af	Sarapiquí	wf-T
C10	-83.750	10.460	41	Af	Tortuguero	wf-T
C11	-83.438	10.460	0	Af	Tortuguero	wf-T
C12	-84.063	10.147	1,822	Cf	Puerto Viejo	rf-LM
C13	-83.750	10.147	596	Af	Tortuguero	wf-PM
C14	-83.438	10.147	36	Af	Pacuare	wf-T
C15	-83.750	9.835	1,104	Cf	Reventazón	wf-PM
C16	-83.438	9.835	1,163	Af	Pacuare	wf-PM
C17	-83.125	9.835	515	Af	Estrella	wf-PM
C18	-83.438	9.523	2,597	Cw	Telire	wf-PM
C19	-83.125	9.523	740	Cw	Telire	rf-M
P1	-85.625	11.084	199	Aw	Sapoa	wf-PM
P2	-85.625	10.772	192	Aw	Tempisque	mf-PM
P3	-85.313	10.772	894	Aw	Tempisque	wf-PM
P4	-85.625	10.460	102	Aw	Tempisque	mf-PM
P5	-85.313	10.460	135	Aw	Tempisque	mf-PM
P6	-85.000	10.460	377	Aw	Bebedero	mf-PM
P7	-85.625	10.147	504	Aw	Tempisque	mf-T
P8	-85.313	10.147	28	Aw	Nicoya Península	mf-PM
P9	-85.000	10.147	88	Aw	Nicoya Península	mf-PM
P10	-84.688	10.147	1423	Aw	Barranca	wf-PM
P11	-84.375	10.147	1475	Cw	Grande Tárcoles	mf-PM
P12	-85.313	9.835	112	Aw	Nicoya Península	mf-PM
P13	-85.000	9.835	297	Aw	Nicoya Península	mf-T
P14	-84.688	9.835	0	Am	Jesús María	mf-T
P15	-84.375	9.835	769	Aw	Grande Tárcoles	wf-PM
P16	-84.063	9.835	1529	Aw	Grande Tárcoles	rf-LM
P17	-84.375	9.523	8	Am	Parrita	mf-T
P18	-84.063	9.523	398	Cw	Naranjo	wf-T
P19	-83.750	9.523	2,012	Am	Grande Térraba	rf-LM
P20	-83.750	9.211	325	Af	Grande Térraba	mf-T
P21	-83.438	9.211	484	Am	Grande Térraba	wf-T
P22	-83.125	9.211	2,037	Am	Grande Térraba	rf-LM
P23	-83.438	8.899	33	Af	Grande Térraba	wf-T
P24	-83.125	8.899	582	Am	Grande Térraba	wf-T
P25	-82.813	8.899	1,223	Am	Cabagra	wf-PM
P26	-83.438	8.586	86	Af	Osa Península	wf-T
P27	-83.125	8.586	24	Af	Esquinas	wf-T

Note. The geographic coordinates and elevation are shown in decimal degrees and meters above sea level (m a.s.l.), respectively. Climate classification is based in the Köppen–Geiger classification system. For each station, the related watershed and the Holdridge life zone are also included. CFSR = Climate Forecast System Reanalysis.

<sup>a</sup>Köppen-Geiger code: Aw = tropical wet and dry; Am = tropical trade-wind littoral; Af = tropical rainforest; Cf = humid; Cw = tropical highland.

<sup>b</sup>Holdridge life zones: rf-LM = lower montane rainforest; rf-M = montane rainforest; mf-PM = premontane moist forest; wf-PM = premontane wet forest; mf-T = tropical moist forest; wf-T = tropical wet forest.

based on the availability of annual records of P, PET, and AET during a minimum of 15 years. The sites were separated into the following regions: Northern Pacific region, NP (P2, P3, P5, P7, and P8), Pacific coast (P9 and P20), Caribbean lowlands, CL (C3, C4, C5, C6, C8, C9, C10, C11, C13, C14, and C17), and Caribbean and Pacific mountainous regions, CM and PM, respectively (C2, C7, C12, C15, C16, C18, C19, P6, P10, P11, P19, P21, and P25).

PET is generally understood to refer to the maximum rate of evaporation from a large area covered completely and uniformly by actively growing vegetation with adequate moisture at all times (Brutsaert, 2005). Brutsaert (2015) suggested that PET can be calculated using the Priestley and Taylor equation (Priestley & Taylor, 1972), which does not include wind speed and vapor pressure effects. We used this equation during the period 1989–2005, as follows:

$$PET = \alpha_e \frac{\Delta}{\Delta + \gamma} Q_{ne}, \quad (1)$$

where PET is the rate of potential evapotranspiration (mm/day),  $\alpha_e$  is a constant (1.26),  $Q_{ne}$  is the net solar radiation ( $J/m^2$  day),  $\Delta$  is of the slope of the saturation vapor density curve, and  $\gamma$  is the psychrometric constant.

An evaluation of precipitation P, AET, and PET data was performed using observed data records and Moderate Resolution Imaging Spectroradiometer (MODIS) PET and AET products (Moderate Resolution Imaging Spectroradiometer, MODIS, 2014). The results of this evaluation are included as supplementary material (Figures S1–S4). P data retrieved from the CFSR archives were evaluated using observed P data as shown in Figure S1 (Fuka et al., 2013; Worqlul et al., 2015). The long-term mean annual P (MAP, mm/year as shown in Figure 1b) data were compiled using 276 sites with at least 10 years of continuous records, where >80% falls in the period 1960–2000 (Sánchez-Murillo & Birkel, 2016). Ten CFSR sites (C2, C3, C8, C16, C19, P2, P8, P17, P21, and P27) were compared to the P records available at the National Meteorology Institute of Costa Rica (IMN) database (available at <https://www.imn.ac.cr>).

When CFSR rainfall data were compared to the mean value of rain gauge data shown in Figure S1 and the IMN observations, we found that the sites were too low for the Caribbean slope and too high for regions such as the Central Valley and the NP slope. However, CFSR rainfall sites captured the gauged pattern over the evaluated time period, as indicated by the good correlation between the CFSR sites (Figure S4a) and the observed data ( $r = .84-.95$ ,  $p < .05$ ). Such a relationship allowed further adjustment of the data to fit the observations by adopting a spatial bias (error) correction method (Terink, Hurkmans, Torfs, & Uijlenhoet, 2009; Vernimmen, Hooijer, Mamun, & van Dijk, 2012). The correction was applied using the following expression:

$$P_{corrected} = P_i - P_{error}, \quad (2)$$

where  $P_i$  is the precipitation recorded in year  $i$  within the time period 1989–2005 and the  $P_{error}$  is the average error in the MAP calculated in the time period 1989–2005 with CFSR P and MAP data as reported by Sánchez-Murillo and Birkel (2016).

The calculations of PET were evaluated using MODIS (2014) estimations and the same 10 IMN sites used to evaluate the P data (Figures S2 and S4b). Solar radiation retrieved from IMN was

complemented with the data reported by Wright (2008). CFSR temperature data were not corrected because the lapse rate calculated using CFSR temperatures ( $-4.0$  °C/km) was in good agreement with the  $-5.4$  °C/km value used by Sánchez-Murillo et al. (2013). Therefore, the data were directly used to calculate PET (Equation 1).

To evaluate the LandFlux-EVAL AET product, the relative annual bias in AET was calculated using MODIS (2014) sites as a reference product (see Figure S3). For sites with no available LandFlux-EVAL product, AET values were calculated using the AET/PET ratio of the nearest site. The average AET/PET ratios across Costa Rica were in the range of 58%–90%. For 10 catchments (C2, C3, C13, C15, C18, P5, P8, P9, P10, and P21; Table 1), mean annual water balance runoff sites were computed and compared to gauged runoff available from the Global Runoff Data Center database (Global Runoff Data Centre, 2015) as shown in Figure S4c. The latter comparison was based on the assumption that runoff can be calculated as  $Q = P - AET$  ( $Q =$  runoff) under negligible storage changes ( $\Delta S = 0$ ).

CFSR PET and LandFlux-EVAL data were not corrected and were used directly for the hydroclimatic analysis, because MODIS (2014) PET data was found to be positively correlated with the PET values calculated with Equation 1 using the CFSR data (Figure S4b). The strongest correlation with PET was found for the sites located in the Caribbean slope ( $r = .96$ ). Runoff values calculated using LandFlux-EVAL AET sites also showed strong correlations for both slopes with gauging observations ( $r = .99$ ). When the AET and PET data sets were compared with the MODIS product, relative annual biases were in the range  $-0.30$  to  $+0.70$  and  $-0.33$  to  $+0.36$  mm/year, respectively (Figures S2 and S3). Overall, the biases between the LandFlux-EVAL and MODIS AET data are similar to the mean absolute biases reported for MODIS ET versus tower ET measurements (Mu, Zhao, & Running, 2011), whereas PET biases found between the CFSR and MODIS PET are similar to those found by Lu, Sun, McNulty, and Amatya (2005) between different PET calculation methods. A summary of the P, PET, and AET data used in the analysis is shown in Table S1, including the calculated bias for each hydroclimatic component and the  $P_{error}$ .

## 2.4 | Analysis of ecohydrological conditions

The CFSR sites located both on the Caribbean and Pacific slopes were classified according to their annual partitioning of P into AET and Q using the Budyko framework. The average annual dryness index ( $\Phi$ ), defined as the ratio of PET to P, and the average evaporative index, calculated as the ratio of AET to P, were plotted within the Budyko boundary conditions and compared to the original Budyko curve (Equation 3) for the time period 1989–2005:

$$\frac{AET}{P} = \left[ \phi \tanh\left(\frac{1}{\phi}\right) (1 - \exp^{-\phi}) \right]^{0.5}. \quad (3)$$

The coupled water–energy balance framework developed by Tomer and Schilling (2009) was used to assess if unused available energy and water were related to climate and/or to land management. It was assumed that in the long term, the basin AET is mainly limited by water supply P and energy supply PET, which considered together determine a hydroclimatic state space (Renner et al., 2012). Therefore, the observed changes in the long-term hydrological conditions can be

assumed to be caused by either climatic change or changes in the basin conditions such as land use and vegetation cover (Tomer & Schilling, 2009). The unused available energy (U or energy excess) and water (W or water excess) were calculated at each site, respectively, as follows:

$$U = 1 - \frac{\text{AET}}{\text{PET}}, \quad (4)$$

$$W = 1 - \frac{\text{AET}}{P} = \frac{Q}{P}. \quad (5)$$

In order to separate the effects of climate and land cover change at each site, the magnitude of change in U ( $\Delta U$ ) and W ( $\Delta W$ ) was calculated for 1989–2005 following Tomer and Schilling (2009), Renner et al. (2012), and Cai, Fraedrich, Sielmann, Guan, and Guo (2016) as follows:

$$\Delta U = -\sum_{i=1989}^{2005} (U_{i+1} - U_i), \quad (6)$$

$$\Delta W = -\sum_{i=1989}^{2005} (W_{i+1} - W_i), \quad (7)$$

where  $U_{i+1} - U_i$  are the annual deviations in U and  $W_{i+1} - W_i$  the annual deviations in W calculated, each summed for the same time period, respectively. Here, we also included the climate change impact hypothesis, relevant for the sensitivity of AET and streamflow to changes in P and PET, where  $\Delta U = -\Delta W$  (Renner & Bernhofer, 2012; Renner et al., 2012). Additionally, we assumed that the long-term catchment mass balances were closed, and therefore, our input data represent average values that include seasonal and shorter term variations in water availability and PET (Freund & Kirchner, 2017). Thus, the magnitudes of change can be used to identify variations in the P/PET ratio, which, in turn, can be linked to climatic changes at the regional scale or to recognize if there are concurrent alterations in climate and vegetation that provoke ecohydrological effects of similar magnitude (Peña-Arancibia et al., 2012; Renner et al., 2012; Tomer & Schilling, 2009). Additionally, a one-sample t test was used to evaluate if the changes in relative W and U were significantly different from the annual average change calculated for each CFSR site ( $\alpha = 0.05$ ) (Renner & Bernhofer, 2012).

Analysis of the hydroclimatic conditions was done introducing two additional concepts: the hydrological resistance and resilience (Carey et al., 2001; Creed et al., 2014). The hydrological resistance is a measure of synchronicity between the partitioning of P into Q in a catchment (Creed et al., 2014). Resilience is a measure of hydrological elasticity (i.e., the degree to which a catchment can return to normal functioning following hydroclimatic perturbations; Carey et al., 2001; Creed et al., 2014). The resistance and resilience at each estimate were calculated using the standard deviation ( $\sigma$ ) in U and W in the time period 1989–2005 as follows:

$$\sigma_U = \sqrt{\frac{1}{n-1} \sum_{i=1}^n (U_i - \bar{U})^2}, \quad (8)$$

$$\sigma_W = \sqrt{\frac{1}{n-1} \sum_{i=1}^n (W_i - \bar{W})^2}, \quad (9)$$

where  $\bar{U}$  and  $\bar{W}$  are the mean values of U and W over the time period 1989–2015. The hydrological resistance was estimated using

the standard deviation of the ratio of Q to P (or W) in a given time period. A relatively small deviation in the dryness index or the ratio of PET to P at sites with high resilience would not result in a significant change in the water use of the catchment (i.e., a significant deviation in the Q to P ratio). The relative magnitude of both deviations (i.e., the  $\sigma_U$  to  $\sigma_W$  ratio) was used to classify a catchment according to its resilience.

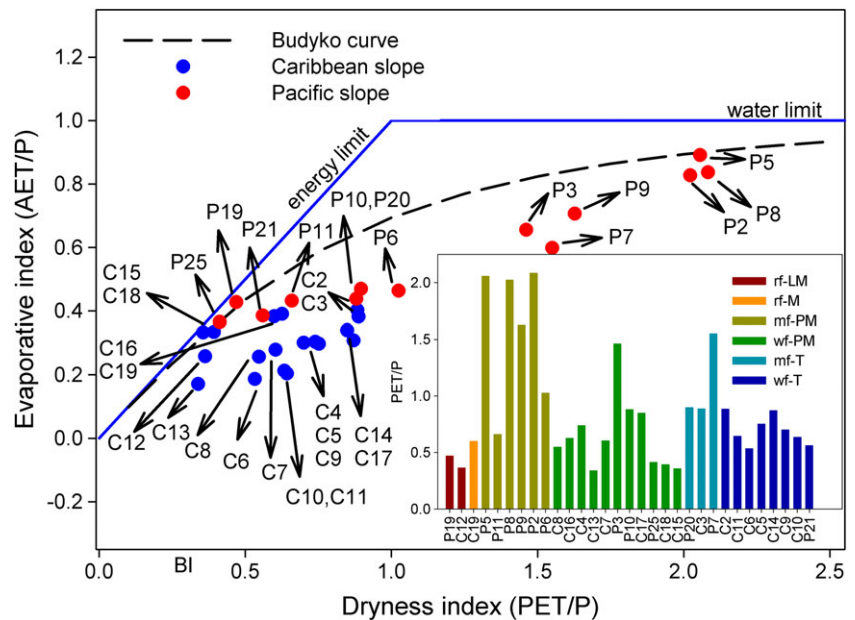
### 3 | RESULTS AND DISCUSSION

#### 3.1 | Budyko analysis and aridity index across different biomes

Within the Budyko boundary conditions (Figure 2a), the sites located on the Pacific slope were water limited, whereas the sites located on the Caribbean slope were mostly energy limited. This delineation is especially clear for the P2, P5, and P8 sites on the NP, which may be explained by the unsynchronized partitioning of P into AET related to the vegetation type of the region (Zhang, Dawes, & Walker, 2001) or by other missing components such as a net change in the storage related to prolonged dry periods (Potter, Zhang, Milly, McMahon, & Jakeman, 2005). For the Pacific slope sites, anthropogenic factors such as the introduction of high water-demanding commercial tree plantations such as teak (*Tectona grandis* L.; Lacombe et al., 2015) and heavy water use/extraction by agriculture and tourism activities may also be linked to observed deviations from equilibrium conditions, but there is still little information available to test this hypothesis for this region. Some sites, such as P3, P7, and P9, also deviated from the equilibrium conditions according to the Budyko framework but could be classified as dry regions (van der Velde et al., 2013). In general, sites that are more water limited share a common climate class (tropical wet and dry climate or Aw, as shown in Table 1) and are located in the NP, exceeding an average dryness of 1.0. Enquist (2002) demonstrated that this biome is extremely sensitive to moisture changes and that small changes in rainfall could cause relatively large changes in its distribution. Therefore, if the observed partitioning of P into AET and Q in the NP continues, this could lead to poor hydrological conditions for biomes such as the moist forest, especially those located in premontane regions (Karmalkar, Bradley, & Diaz, 2008).

Unlike the sites on the Pacific slope, the energy-limited Caribbean domain appears to be related to the relatively greater precipitation amounts throughout the year. For example, C12, located in the central mountainous region, was in equilibrium conditions and can be classified as humid with a relatively high-water yield (Creed et al., 2014). The more humid sites on the Caribbean slope correspond to the tropical rainforest climate class Af (see Table 1) and are located close to the Caribbean coast, where wet forests are abundant. Overall, the observed hydrological conditions can be considered good to sustain the wet and rainforests of this biome. However, it is imperative to quantify the water storage changes in these catchments and evaluate their impacts within the Budyko framework (Li, Pan, Cong, Zhang, & Wood, 2013), especially in areas with complex topographic features that significantly affect the long-term average annual evapotranspiration or ET (Shao, Traylen, & Zhang, 2012).

**FIGURE 2** (a) The distribution of the 31 CFSR estimates within the Budyko boundary conditions. Estimates were classified according to the location on the Caribbean (blue dots) and Pacific (red dots) slopes. The Budyko curve is plotted as a reference. Estimates are labeled using the codes shown in Table 1. (b) The inset shows the average PET/P ratios calculated for the 31 estimates included in the ecohydrological analysis (1989–2005). The estimates were classified using the Holdridge life zones system shown in Table 1. CFSR = Climate Forecast System Reanalysis; P = precipitation; PET = potential evapotranspiration; AET = actual evapotranspiration



In terms of the PET/P ratio (i.e., aridity index; Figure 2b), the wet rainforests located in premontane and montane areas showed smaller PET/P ratios (i.e., values smaller than one related to water limitation) than those biomes located in the Pacific and Caribbean coastal regions. This difference is likely related to the thermal regimes, vegetation types, and water availability. The relationship between the PET/P ratios and the mean annual temperature resulted in a significant correlation for the Caribbean ( $n = 18$ ;  $r = .524$ ,  $p = .025$ ) and Pacific ( $n = 13$ ;  $r = .901$ ,  $p < .01$ ) slopes. The sites located at a relatively high elevation (1,500–2,500 m a.s.l.) such as C12, C16, C18, P11, and P21 showed small PET/P ratios, which are related to the relatively lower MAT and higher  $P$  values. The less-dense vegetated biomes present on the Pacific slope and the relatively low  $P$  values (1600–2000 m) of the sites such as P3, P5, P8, and P9 explain the relatively larger PET/P ratios. On the Caribbean slope, the higher PET/P resulted for C3, C4, and C17 (0.74–0.89), but these values are similar to the sites of this region.

In general, the gross primary production fluctuations across the globe are mostly controlled by  $P$  and strongly coupled with ET (Zhang et al., 2016). Therefore, the environmental responses of carbon fluxes to water conditions can be estimated by the ET fluxes (Heimann et al., 1998; Ito & Oikawa, 2000; Wohl et al., 2012). If the drying pattern observed in the NP will continue in the future, these biomes are likely to be affected by low water availability scenarios and to suffer water stress.

### 3.2 | Ecohydrological resistance and resilience analysis

The mean relative water excess ( $\bar{W}$ ) and relative energy excess ( $\bar{U}$ ) for the time period 1989–2005 (Figure 3a) also showed a clear separation between the Caribbean and the Pacific slopes related to the greater relative water excess on the Caribbean slope. The sites on the Pacific slope can be further divided into two subtypes: lower relative energy excess for the Southern Pacific and some premontane sites such as P11, P19, P21, and P25 and high water usage for the NP such as P2, P5, P6, P8, and P9, with  $W$  values ranging from 53% to 63% and

11% to 29%, respectively. These  $\bar{W}$  separation results also show that the lower and premontane moist forests situated in the NP can be severely affected by changes in water availability driven by precipitation changes related to El Niño Southern Oscillation (ENSO) and resulting seasonal droughts that can amplify the tree mortality rates in tropical forests (Chazdon et al., 2005).

In terms of resistance and resilience, the NP slope showed high hydrological resistance because of the high relative deviation of the calculated water excess (Carey et al., 2001). For sites such as P2, P5, and P8, the standard deviation in the water excess was in the range of 29%–33%. Such a range means that the premontane moist forests of this region suffered a deficit in water availability within the period 1989–2005. The results also indicate poor synchronicity in the partitioning of  $P$  into AET and  $Q$  (Creed et al., 2014) and showed low hydrological resilience conditions as small deviations in the energy excess resulted in large deviations in the water excess. Therefore, catchments in these areas showed a minimal ability to sustain the partitioning of  $P$  into AET and  $Q$  consistently as climate varies and to maintain the expected precipitation–discharge relations in light of changing inputs (Carey et al., 2001; Hickel & Zhang, 2006). In contrast, the Southern Pacific and Caribbean slopes showed better ecohydrological conditions because of their relatively small deviations in water excess of 8%–19% and 2%–9%, respectively, and similar deviations in energy and water excess (i.e., high resilience conditions). This finding can be explained with the relatively similar partitioning of  $P$  into AET and  $Q$  that these regions share with the Caribbean slope (Figure 2).

### 3.3 | Forest cover and direction of change in $U$ and $W$

Between 1987 and 2005, the conservation areas located in the Caribbean slope such as ACTO, ACLA-C, and ACHN were affected by negative changes in forest cover in the range  $-3.66\%$  to  $-1.23\%$ , whereas conservation areas such as ACT and ACOPAC, situated on the Pacific slope, showed a positive change in forest cover with values between

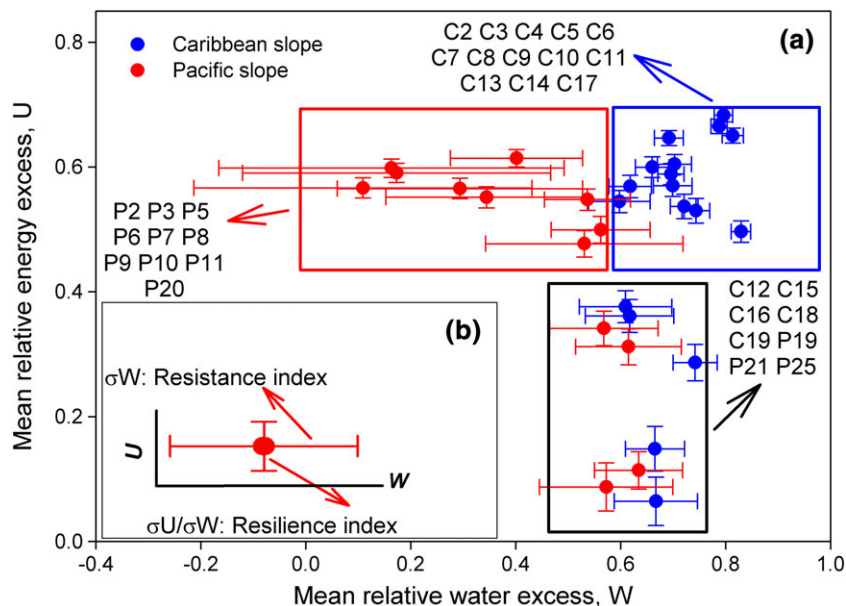


**FIGURE 3** (a) Mean relative energy excess ( $\bar{U}$ ) and mean relative water excess ( $\bar{W}$ ) calculated for the 31 CFSR estimates (1989–2005) following the Tomer–Schilling framework. Estimates were further classified according to the location in the Caribbean (blue dots) and Pacific (red dots) slopes. Error bars in  $U$  and  $W$  represent  $\pm 1\delta$ . (b) Graphical representation of resistance and resilience metrics. The resistance and resilience indexes are calculated using Equations 8 and 9. CFSR = Climate Forecast System Reanalysis

1.64% and 9.76% (Sánchez-Azofeifa et al., 2002, 2006). As shown in Figure 4, these changes in forest cover were significantly correlated with the mean relative change in the water excess or  $\Delta W$  calculated for each conservation area ( $r = -0.929$ ,  $p < .001$ ). The observed relationship between  $\Delta W$  and the mean change in forest cover are inversely correlated by the negative slope shown in Figure 4, which means that the water-limited and less resilient NP was afforested during the time period 1989–2005. When the changes in the forest cover were compared with the mean change in the energy excess or  $\Delta U$ , the observed relationship was also inversely proportional but relatively weak for the ACTO, ACLA-C, ACHN, ACLA-P, and ACCVC conservation areas ( $r = -0.900$ ,  $p < .1$ ). It is apparent that the ACOPAC and ACT conservation areas did not follow the observed trend of the other conservation areas because the greater changes in forest cover led to relatively the same changes in the energy excess (Figure 4). This observation might be related with the climatic variations and a decrease in annual average P that could have affected the water-limited Pacific region. Based on the Tomer–Schilling framework, a decrease in the mean P would leave less water for both ET and Q, which would result also in positive

changes in  $U$  (increasing energy excess) and in negative changes in  $W$  (decreasing water excess; Renner et al., 2012; Tomer & Schilling, 2009). At the local scale, there is a need to assess if the observed mean  $W$  and  $U$  were affected by significant changes in P or PET, besides the changes in forest cover, and to determine if there were simultaneous significant changes in  $U$  and  $W$  (Renner & Bernhofer, 2012; Renner, Brust, Schwärzel, Volk, & Bernhofer, 2014).

The overall trend in the direction of changes in  $U$  and  $W$  shown in Figure 5a and calculated following Tomer and Schilling (2009) revealed that some CFSR sites located in the NP such as P2 and P3 were affected by a significant decrease in  $W$  in the time period 1989–2005 ( $p < .05$ ). This result was also found for the P6 and P11 sites that are located in the ACA-T and ACCVC conservation areas, respectively. On the Caribbean slope, the sites that are located in the northern CL such as C2, C4, C7, and C8 also showed significant changes in water access with values between  $-2.4\%$  and  $-6.6\%$ , whereas those sites located closed to the Caribbean coast such as C6, C10, C11, and C14 showed no significant change in  $W$ . It appears that hydrological conditions present in these regions are related with ongoing climatic change

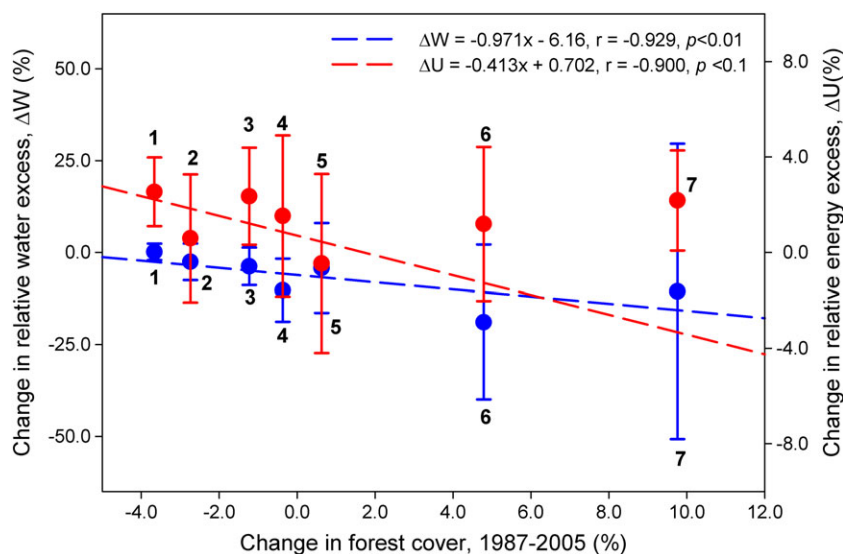


**FIGURE 4** Scatter plot showing the relationship between the mean relative change in the water excess ( $\Delta W$ , blue dots), the mean relative change in the energy excess ( $\Delta U$ , red dots), and the mean change in the forest cover of the conservation areas shown in Figure 1. Only conservation areas with at least three CFSR estimates located within their limits were used to calculate the mean values and included in the analysis. Error bars in  $\Delta U$  and  $\Delta W$  were calculated using  $1\delta$ . Conservation areas were numbered following the description shown in Figure 1 as (1) ACTO, (2) ACLA-C, (3) ACHN, (4) ACLA-P, (5) ACCVC, (6) ACOPAC, and (7) ACT

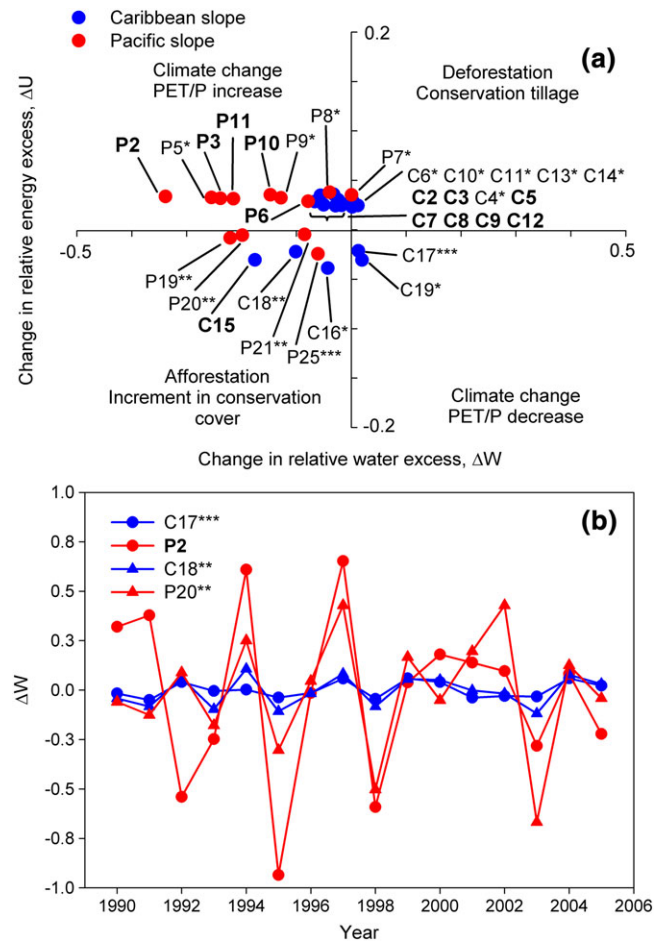


**FIGURE 5** (a) Ecohydrological conditions and changes in climate and land use calculated for the estimates located in the Caribbean (blue dots) and the Pacific slopes (red dots). Using the *t* test results, labels of the sites with significant ( $p < .05$ ) changes in both *W* and *U* are shown in bold. Other estimates were classified as no significant change in  $\Delta W$  but significant change in  $\Delta U$  (\*), no significant change in  $\Delta U$  but significant change in  $\Delta W$  (\*\*), and no significant change in  $\Delta W$  nor  $\Delta U$  (\*\*\*). (b) Time series plot comparing the year-to-year deviations in the relative water excess for C17 and C18 (Caribbean slope) and P2 and P20 (Pacific slope). *P* = precipitation; *PET* = potential evapotranspiration

due to increasing *PET* to *P* ratios in the time period 1989–2005 that led to a decrease in water excess of ~2.3% to 34%.

In the NP, the average precipitation deficit, with respect to historical MAP shown in Figure 1b (Sánchez-Murillo & Birkel, 2016), was 192 mm/year, which explains the increase in the *PET/P* ratios. Hidalgo et al. (2013) calculated precipitation changes with a distinct drying pattern for the Pacific corridor of Central America, with maximum values of around 5%–10%, which indicates that these conditions could significantly affect the distribution of biomes such as the lower and premontane forests of this region (Enquist, 2002). However, sites P5, P7, P8, and P9 in the NP could not be linked with these ongoing changes in *P* patterns. These sites share two characteristics: their location within the ACT conservation area, with a reported change of 9.76% in forest cover, and their situation inside watersheds that drain across the Nicoya Peninsula. They also had high standard deviations in *W* or high resistance values as shown in Figure 3a, with values of approximately 0.30. These results might be related with the observed

changes in the forest cover because in water-limited basins (i.e., with *PET* to *P* ratios close to 1 as shown in the Budyko analysis for these subregions), the separation of impacts from climate and land use is less certain and even small basin changes (e.g., in vegetation) can greatly affect the hydrological responses (Renner et al., 2012; Wang & Hejazi, 2011).

These large effects on hydrological responses were evident in the year-to-year deviations in *W* estimated for P2 (Figure 5B), especially in the time period 1989–1998 when *W* had high variability. Unlike the NP, these effects were not observed in C17, which is located in the southern CL (Figure 5b). In the time period 1963–2003, Alfaro (2002) reported that the annual total precipitation divided by the number of wet days (precipitation >1.0 mm) showed a positive significant trend or an increase in the precipitation of this region. However, no change in *W* was detected using the C17 and C18 sites that can be associated with these changes in the precipitation of this region. Overall, their relative low variability in *W* shown in Figure 5b is related with the consistent partitioning of *P* into *AET* and *Q* and the high hydrological resilience of this region.

Although C18 in the CM and P20 on the Southern Pacific slope also showed significant changes in *W* (Figure 5a and 5b), no significant changes were observed in *U*, unlike those sites in the NP. Therefore, there is no evidence of afforestation effects for these regions. The same is true for the P25 estimate where no significant changes in *U* or *W* were found. Then, only one site, C15 (in the ACCVC conservation area and at the border of a protected area), was associated with a decrease in *Q* or an increase in forest cover. Hence, the premontane tropical wet forest situated in this region benefits from the local hydroclimatic conditions and the presence of protected areas that lead to a more efficient use of the energy and water (i.e., a synchronized decrease in the *U* and *W*).

## 4 | CONCLUSIONS

Hydroclimatic conditions and ecohydrological resistance and resilience states were evaluated for Costa Rica in the time period 1989–2005 using the Budyko and Tomer–Schilling frameworks. Within the Budyko boundary conditions, the sites located in the Pacific slope showed a tendency to be water limited, whereas the sites located in the Caribbean slope are energy limited. Some sites located on the Pacific slope showed unsynchronized partitions of *P* into *AET* and *Q* related with a precipitation deficit during the studied time period. The Pacific sites were further divided into two types: high resilience sites, with similar deviations in the energy excess *U* and water excess *W*, and high resistance, with high deviations in *W*. Mean  $\Delta W$  values were significantly correlated ( $p < .01$ ) with the mean change in forest cover observed in the conservation areas in the time period 1987–2005. In terms of energy, the relationship between the mean  $\Delta U$  values and the mean change in forest cover was relative weak ( $p < .1$ ) and was only observed at the conservation areas located in energy-limited regions. Using the Tomer–Schilling framework and the magnitude of  $\Delta U$  and  $\Delta W$  during 1989–2005, some sites located in the NP and CL showed a significant increase in the *PET* to *P* ratios ( $p < .05$ ), respectively, due to ongoing climatic change effects, namely, changes in the

precipitation inputs. For the Nicoya Peninsula, due to the high standard deviations in *W* or high resistance values, our analysis could not identify changes for the water-limited sites located in the ACT conservation area. The calculated resistance values suggest that the biomes located in the NP region such as the lower and premontane moist forests are especially susceptible to observed changes in the ecohydrological conditions considered in this study, especially to water-limited conditions, low resilience, and high variability in *W*. In contrast, the wet rainforests located on the southern Pacific and Caribbean slope (coastal zones) are under the influence of more stable ecohydrological conditions due to the high water availability and high hydrological resilience.

Our findings should be incorporated into the development of effective conservation and management strategies for catchments and tropical forests in Costa Rica. For example, the national and regional water administrators should use the hydrological susceptibility to droughts of regions such as the NP slope to adopt effective management policies that optimize water use efficiency and water storage according to the region resilience. Finally, further research that includes longer time periods and data sets with greater spatial and temporal resolution would help to broaden the outcomes of this study to regions that lack hydrological information.

## ACKNOWLEDGEMENTS

This work was supported by the World Bank and National University of Costa Rica partial PhD scholarship to G. E. H. in the Climate Change and Natural Resources Management doctorate program at DOCINADE (San José, Costa Rica). G. E. H. and R. S. M. also thank the Research Office at the National University of Costa Rica for its support through the Grants SIA-0482-13 and SIA-0101-14.

## REFERENCES

- Alfaro, E. J. (2002). Some characteristics of the annual precipitation cycle in Central America and their relationships with its surrounding tropical oceans. *Topics in Meteorology and Oceanography*, 9(2), 88–103.
- Allen, C. D., Macalady, A. K., Chenchouni, H., Bachelet, D., & McDowell, N. (2010). A global overview of drought and heat-induced tree mortality reveals emerging climate change risks for forests. *Forest Ecology and Management*, 259(4), 660–684. <https://doi.org/10.1016/j.foreco.2009.09.001>
- Brutsaert, W. (2005). *Hydrology—An introduction*. New York: Cambridge University Press. <https://doi.org/10.1017/CBO9780511808470>
- Brutsaert, W. (2015). A generalized complementary principle with physical constraints for land-surface evaporation. *Water Resources Research*, 51, 1–7. <https://doi.org/10.1002/2015WR017720>
- Budyko, M. I. (1974). *Climate and life*. New York: Academic Press.
- Cai, D., Fraedrich, K., Sielmann, F., Guan, Y., & Guo, S. (2016). Land-cover characterization and aridity changes of South America (1982–2006): An attribution by ecohydrological diagnostics. *Journal of Climate*, 29, 8175–8189. <https://doi.org/10.1175/JCLI-D-16-0024.1>
- Carey, S. K., Tetzlaff, D., Seibert, J., Soulsby, C., Buttle, J., Laudon, H., ... Pomeroy, J. W. (2001). Inter-comparison of hydro-climatic regimes across northern catchments: Synchronicity, resistance and resilience. *Hydrological Processes*, 24, 3591–3602. <https://doi.org/10.1002/hyp.7880>
- Chazdon, R. L., Redondo-Brenes, A., & Vilchez-Alvarado, B. (2005). Effects of climate and stand age on annual tree dynamics in tropical second-growth rain forests. *Ecology*, 86(7), 1808–1815. <https://doi.org/10.1890/04-0572>
- Condit, R., Pérez, R., & Daguerre, N. (2010). *Trees of Panama and Costa Rica*. New Jersey: Princeton University Press. <https://doi.org/10.1515/9781400836178>
- Creed, I. F., Spargo, A. T., Jones, J. A., Buttle, J. M., Adam, M. B., Beall, F. D., ... Yao, H. (2014). Changing forest water yields in response to climate warming: Results from long-term experimental watershed sites across North America. *Global Change Biology*, 20, 3191–3208. <https://doi.org/10.1111/gcb.12615>
- De Fries, R., Karanth, K. K., & Pareeth, S. (2010). Interactions between protected areas and their surroundings in human-dominated tropical landscapes. *Biological Conservation*, 143, 2870–2880. <https://doi.org/10.1016/j.biocon.2010.02.010>
- Donohue, R., Roderick, M. L., & McVicar, T. R. (2007). On the importance of including vegetation dynamics in Budyko's hydrological model. *Hydrology and Earth System Science*, 11, 983–999. <https://doi.org/10.5194/hess-11-983-2007>
- Du, C., Sun, F., Yu, J., Liu, X., & Chen, Y. (2015). New interpretation of the role of water balance in an extended Budyko hypothesis in arid regions. *Hydrology and Earth System Science*, 12, 11013–11052. <https://doi.org/10.5194/hessd-12-11013-2015>
- Enquist, C. A. F. (2002). Predicted regional impacts of climate change on the geographical distribution and diversity of tropical forests in Costa Rica. *Journal of Biogeography*, 29, 519–534. <https://doi.org/10.1046/j.1365-2699.2002.00695>
- Feeley, K. J., Hurtado, J., Saatchi, S., Silman, M. R., & Clark, D. B. (2013). Compositional shifts in Costa Rican forests due to climate-driven species migrations. *Global Change Biology*, 19, 3472–3480. <https://doi.org/10.1111/gcb.12300>
- Findell, K. L., & Knutson, T. R. (2006). Weak simulated extratropical responses to complete tropical deforestation. *Journal of Climate*, 19, 2835–2850. <https://doi.org/10.1175/JCLI3737.1>
- Fisher, J. B., Malhi, Y., Bonal, D., Da Rocha, H. R., De Araújo, A. C., Gamo, M., ... Von Randow, C. (2009). The land-atmosphere water flux in the tropics. *Global Change Biology*, 15, 2694–2714. <https://doi.org/10.1111/j.1365-2486.2008.01813>
- Freund, E. R., & Kirchner, J. W. (2017). A Budyko framework for estimating how spatial heterogeneity and lateral moisture redistribution affect average evapotranspiration rates as seen from the atmosphere. *Hydrology and Earth System Science*, 21, 217–233. <https://doi.org/10.5194/hess-21-217-2017>
- Fuka, D. R., Walter, M. T., MacAlister, C., Degaetano, A. T., Steenhuis, T. S., & Easton, Z. M. (2013). Using the Climate Forecast System Reanalysis as weather input data for watershed models. *Hydrological Processes*, 28(22), 5613–5623. <https://doi.org/10.1002/hyp.10073>
- Giorgi, F. (2006). Climate change hot-spots. *Geophysical Research Letters*, 33, L08707. <https://doi.org/10.1029/2006GL025734>
- Global Runoff Data Centre. 2015. Global runoff Data Base. Global Runoff Data Centre. Koblenz, Federal Institute of Hydrology (BfG). [http://www.bafg.de/GRDC/EN/03\\_dtprcdts/32\\_LTMM/longtermmonthly\\_node.html](http://www.bafg.de/GRDC/EN/03_dtprcdts/32_LTMM/longtermmonthly_node.html)
- Greve, P., Gudmundsson, L., Orłowski, B., & Seneviratne, S. I. (2015). The Budyko framework beyond stationarity. *Hydrology and Earth System Science*, 12, 6799–6830. <https://doi.org/10.5194/hessd-12-6799-2015>
- Hassler, N., Werth, D., & Avissar, R. (2009). Effects of tropical deforestation on global hydroclimate: A multimodel ensemble analysis. *Journal of Climate*, 22, 1121–1141. <https://doi.org/10.1175/2008jcli2157.1>
- Heimann, M., Esser, G., Haxeltine, A., Kaduk, J., Kicklighter, D. W., Knorr, W., ... Würth, G. (1998). Evaluation of terrestrial carbon cycle models through simulations of the seasonal cycle of atmospheric CO<sub>2</sub>: First results of a model intercomparison study. *Global Biogeochemical Cycles*, 12(1), 1–24. <https://doi.org/10.1029/97GB01936>
- Hickel, K., & Zhang, L. (2006). Estimating the impact of rainfall seasonality on mean annual water balance using a top-down approach. *Journal of Hydrology*, 331, 409–424. <https://doi.org/10.1016/j.jhydrol.2006.05.028>

- Hidalgo, H. G., Amador, J. A., Alfaro, E. J., & Quesada, B. (2013). Hydrological climate change projections for central America. *Journal of Hydrology*, 495, 94–112. <https://doi.org/10.1016/j.jhydrol.2013.05.004>
- Holdridge, L. R. (1978). *Ecología Basada en Zonas de Vida*. San José, Costa Rica: IICA.
- Imbach, P., Molina, L., Locatelli, B., Rounsard, O., Ciais, P., Corrales, L., & Mahé, G. (2010). Climatology-based regional modelling of potential vegetation and average annual long-term runoff from Mesoamerica. *Hydrology and Earth System Science*, 14, 1801–1817. <https://doi.org/10.5194/hess-14-1801-2010>
- Ito, A., & Oikawa, T. (2000). A model analysis of the relationship between climate perturbations and carbon budget anomalies in global terrestrial ecosystems: 1970 to 1997. *Climate Research*, 15, 161–183. <https://doi.org/10.3354/cr015161>
- Karmalkar, A. V., Bradley, R. S., & Diaz, H. F. (2008). Climate change scenario for Costa Rican montane forests. *Geophysical Research Letters*, 35, L11702. <https://doi.org/10.1029/2008GL033940>
- Karmalkar, A. V., Bradley, R. S., & Diaz, H. F. (2011). Climate change in Central America and Mexico: Regional climate model validation and climate change projections. *Climate Dynamics*, 37, 605–629. <https://doi.org/10.1007/s00382-011-1099-9>
- Kottek, M., Grieser, J., Beck, C., Rudolf, B., & Rubel, F. (2006). World map of the Köppen-Geiger climate classification updated. *Meteorologische Zeitschrift*, 15(3), 259–263. <https://doi.org/10.1127/0941-2948/2006/0130>
- Lacombe, G., Ribolzi, O., de Rouw, A., Pierret, A., Latschak, K., Silvera, N., ... Valentin, C. (2015). Afforestation by natural regeneration or by tree planting: Examples of opposite hydrological impacts evidenced by long-term field monitoring in the humid tropics. *Hydrology and Earth System Science Discussions*, 12, 12615–12648. <https://doi.org/10.5194/hessd-12-12615-2015>
- Li, D., Pan, M., Cong, Z., Zhang, L., & Wood, E. (2013). Vegetation control on water and energy balance within the Budyko framework. *Water Resources Research*, 49, 1–8. <https://doi.org/10.1002/wrcr.20107>
- Lu, J., Sun, G., McNulty, S. G., & Amatya, D. M. (2005). A comparison of six potential evapotranspiration methods for regional use in the southeastern United States. *Journal of the American Water Resources Association*, 41(3), 621–633. <https://doi.org/10.1111/j.1752-1688.2005.tb03759.x>
- Magaña, V., Amador, J. A., & Medina, S. (1999). The midsummer drought over Mexico and Central America. *Journal of Climatology*, 12, 1577–1588. [https://doi.org/10.1175/1520-0442\(1999\)012<1577:TMDOMA>2.0.CO;2](https://doi.org/10.1175/1520-0442(1999)012<1577:TMDOMA>2.0.CO;2)
- Maldonado, T., Alfaro, E., Fallas-López, B., & Alvarado, L. (2013). Seasonal prediction of extreme precipitation events and frequency of rainy days over Costa Rica, Central America, using canonical correlation analysis. *Advances in Geosciences*, 33, 41–52. <https://doi.org/10.5194/adgeo-33-41-2013>
- Maurer, E. P., Adam, J. C., & Wood, A. W. (2009). Climate model based consensus on the hydrologic impacts of climate change to the Rio Lempa basin of Central America. *Hydrology and Earth System Science*, 13, 183–194. <https://doi.org/10.5194/hess-13-183-2009>
- Misra, V., Pantina, P., Chan, S. C., & DiNapoli, S. (2012). A comparative study of the Indian summer monsoon hydroclimate and its variations in three reanalyses. *Climate Dynamics*, 39, 1149–1168. <https://doi.org/10.1007/s00382-012-1319-y>
- Moderate Resolution Imaging Spectroradiometer (MODIS). 2014. Global evapotranspiration project (MOD16) from the numerical terradynamic simulation Group, Univ. of Montana. <http://www.ntsug.umt.edu/project/mod16>
- Mu, Q., Zhao, M., & Running, S. W. (2011). Improvements to a MODIS global terrestrial evapotranspiration algorithm. *Remote Sensing of Environment*, 115, 1781–1800. <https://doi.org/10.1016/j.rse.2011.02.019>
- Mueller, B., Hirschi, M., Jimenez, C., Ciais, P., Dirmeyer, P. A., Dolman, A. J., ... Seneviratne, S. I. (2013). Benchmark products for land evapotranspiration: LandFlux-EVAL multi-data set synthesis. *Hydrology and Earth System Science*, 17, 3707–3720. <https://doi.org/10.5194/hess-17-3707-2013>
- Peña-Arancibia, J. L., van Dijk, A. I. J. M., Guerschman, J. P., Mulligan, M., Bruijnzeel, L. A. S., & McVicar, T. R. (2012). Detecting changes in streamflow after partial woodland clearing in two large catchments in the seasonal tropics. *Journal of Hydrology*, 416–417, 60–71. <https://doi.org/10.1016/j.jhydrol.2011.11.036>
- Potter, N. J., Zhang, L., Milly, P. C. D., McMahon, T. A., & Jakeman, A. J. (2005). Effects of rainfall seasonality and soil moisture capacity on mean annual water balance for Australian catchments. *Water Resources Research*, 41, W06007. <https://doi.org/10.1029/2004WR003697>
- Powell, G. V. N., Barborak, J., & Rodriguez, S. M. (2000). Assessing representativeness of protected natural areas in Costa Rica for conserving biodiversity: A preliminary gap analysis. *Biological Conservation*, 93, 35–41. [https://doi.org/10.1016/S0006-3207\(99\)00115-9](https://doi.org/10.1016/S0006-3207(99)00115-9)
- Priestley, C. H. B., & Taylor, R. J. (1972). On the assessment of surface heat flux and evaporation using large-scale parameters (PDF). *Monthly Weather Review*, 100(2), 81–82. [https://doi.org/10.1175/1520-0493\(1972\)100<0081:OTAOSH>2.3.CO;2](https://doi.org/10.1175/1520-0493(1972)100<0081:OTAOSH>2.3.CO;2)
- Renner, M., & Bernhofer, C. (2012). Applying simple water-energy balance frameworks to predict the climate sensitivity of streamflow over the continental United States. *Hydrology and Earth System Science*, 16, 2531–2546. <https://doi.org/10.5194/hess-16-2531-2012>
- Renner, M., Brust, K., Schwärzel, K., Volk, M., & Bernhofer, C. (2014). Separating the effects of changes in land cover and climate: A hydro-meteorological analysis of the past 60 yr in Saxony, Germany. *Hydrology and Earth System Science*, 18, 389–405. <https://doi.org/10.5194/hess-18-389-2014>
- Renner, M., Seppelt, R., & Bernhofer, C. (2012). Evaluation of water-energy balance frameworks to predict the sensitivity of streamflow to climate change. *Hydrology and Earth System Science*, 16, 1419–1433. <https://doi.org/10.5194/hess-16-2531-2012>
- Rhodes, A. L., Guswa, A. J., & Newell, S. E. (2006). Seasonal variation in the stable isotopic composition of precipitation in the tropical montane forests of Monteverde, Costa Rica. *Water Resources Research*, 42, W11402. <https://doi.org/10.1029/2005WR004535>
- Saénz, F., & Durán-Quesada, A. M. (2015). A climatology of low level wind regimes over Central America using a weather type classification approach. *Frontiers in Earth Science*, 3(15), 1–18. <https://doi.org/10.3389/feart.2015.00015>
- Saha, S., Moorthi, S., Pan, H. L., Wu, X., Wang, J., Nadiga, S., ... Goldberg, M. (2010). The NCEP Climate Forecast System Reanalysis. *Bulletin of the American Meteorological Society*, 91(8), 1015–1057. <https://doi.org/10.1175/2010BAMS3001.1>
- Sánchez-Azofeifa, A., Calvo-Alvarado, J. C., Chong, M. M., Castillo, M., Jiménez, V. 2006. Estudio de Monitoreo de Cobertura Forestal De Costa Rica 2005. I. Parte: Clasificación de la Cobertura Forestal con Imágenes Landsat ETM+ 2005. Technical Report FUNDATEC, San José, Costa Rica.
- Sánchez-Azofeifa, A., Foley, S., Hamilton, S., Calvo-Alvarado, J. C., Arroyo, P., Jiménez, V. 2002. Estudio de cambios de Cobertura Forestal de Costa Rica 1997-2000. Technical Report FONAFIFO, San José, Costa Rica.
- Sánchez-Murillo, R., & Birkel, C. (2016). Groundwater recharge mechanisms inferred from isoscapes in a complex tropical mountainous region. *Geophysical Research Letters*, 43(10), 5060–5069. <https://doi.org/10.1002/2016GL068888>
- Sánchez-Murillo, R., Esquivel-Hernández, G., Welsh, K., Brooks, E. S., Boll, J., Alfaro-Solis, R., & Valdés-González, J. (2013). Spatial and temporal variation of stable isotopes in precipitation across Costa Rica: An analysis of historic GNIP records. *Open Journal of Modern Hydrology*, 3(4), 226–240. <https://doi.org/10.4236/ojmh.2013.34027>
- Shao, Q. X., Traylen, A., & Zhang, L. (2012). Nonparametric method for estimating the effects of climatic and catchment characteristics on mean annual evapotranspiration. *Water Resources Research*, 48, W03517. <https://doi.org/10.1029/2010WR009610>

- Tekleab, S., Uhlenbrook, S., Mohamed, Y., Savenije, H. H., Temesgen, M., & Wenninger, J. (2011). Water balance modeling of Upper Blue Nile catchments using a top-down approach. *Hydrology and Earth System Science*, 15, 2179–2193. <https://doi.org/10.5194/hess-15-2179-2011>
- Terink, W., Hurkmans, R. T. W. L., Torfs, P. J. J. F., & Uijlenhoet, R. (2009). Bias correction of temperature and precipitation data for regional climate model application to the Rhine basin. *Hydrology and Earth System Science*, 6, 5377–5413. <https://doi.org/10.5194/hessd-6-5377-2009>
- Tomer, M. D., & Schilling, K. E. (2009). A simple approach to distinguish land-use and climate-change effects on watershed hydrology. *Journal of Hydrology*, 376, 24–33. <https://doi.org/10.1016/j.jhydrol.2009.07.029>
- Van der Velde, Y., Vercauteren, N., Jaramillo, F., Dekker, S. C., Destouni, G., & Lyon, S. W. (2013). Exploring hydroclimatic change disparity via the Budyko framework. *Hydrological Processes*, 28(13), 4110–4118. <https://doi.org/10.1002/hyp.9949>
- Vernimmen, R. R. E., Hooijer, A., Mamenun, A. E., & van Dijk, A. I. J. M. (2012). Evaluation and bias correction of satellite rainfall data for drought monitoring in Indonesia. *Hydrology and Earth System Science*, 16, 133–146. <https://doi.org/10.5194/hess-16-133-2012>
- Wang, D., & Hejazi, M. (2011). Quantifying the relative contribution of the climate and direct human impacts on mean annual streamflow in the contiguous United States. *Water Resources Research*, 47, W00J12. <https://doi.org/10.1029/2010WR010283>
- Waylen, M. E. (1996). Interannual variability of monthly precipitation in Costa Rica. *Journal of Climatology*, 9, 2606–2613. [https://doi.org/10.1175/1520-0442\(1996\)009<2606:IVOMPI>2.0.CO;2](https://doi.org/10.1175/1520-0442(1996)009<2606:IVOMPI>2.0.CO;2)
- Wohl, E., Barros, A., Brunzell, N., Chappell, N. A., Coe, M., Giambelluca, T., ... Ogden, F. (2012). The hydrology of the humid tropics. *Nature Climate Change*, 2, 655–662. <https://doi.org/10.1038/nclimate1556>
- Worqlul, A. W., Collick, A. S., Tilahun, S. A., Langan, S., Rientjes, T. H. M., & Steenhuis, T. S. (2015). Comparing TRMM 3B42, CFSR and ground-based rainfall sites as input for hydrological models, in data scarce regions: The upper Blue Nile Basin, Ethiopia. *Hydrology and Earth System Science*, 12, 2081–2112. <https://doi.org/10.5194/hessd-12-2081-2015>
- Wright, J. (2008). Cálculo y mapeo de la radiación solar directa y difusa en Costa Rica. *UNICIENCIA*, 22, 55–69.
- Zhang, L., Dawes, W. R., & Walker, G. R. (2001). Response of mean annual evapotranspiration to vegetation changes at catchment scale. *Water Resources Research*, 37(3), 701–708. <https://doi.org/10.1029/2000WR900325>
- Zhang, Y., Xiao, X., Guanter, L., Zhou, S., Ciais, P., Joiner, P., ... Stocker, B. D. (2016). Precipitation and carbon-water coupling jointly control the interannual variability of global land gross primary production. *Scientific Reports*, 6, 39748. <https://doi.org/10.1038/srep39748>
- Zhang, S., Yang, H., Yang, D., & Jayawardena, A. W. (2015). Quantifying the effect of vegetation change on the regional water balance within the Budyko framework. *Geophysical Research Letters*, 43, 1140–1148. <https://doi.org/10.1002/2015GL066952>

## SUPPORTING INFORMATION

Additional Supporting Information may be found online in the supporting information tab for this article.

**How to cite this article:** Esquivel-Hernández G, Sánchez-Murillo R, Birkel C, Good SP, Boll J. Hydroclimatic and ecohydrological resistance/resilience conditions across tropical biomes of Costa Rica. *Ecohydrology*. 2017;10:e1860. <https://doi.org/10.1002/eco.1860>